Platinum and palladium on carbon nanotubes

Adjizian, J. J.; De Marco, P.; Suarez-Martinez, I.; El Mel, A. A.; Snyders, R.; Gengler, R. Y. N.; Rudolf, P.; Ke, X.; Van Tendeloo, G.; Bittencourt, C.

Published in:
Chemical Physics Letters

DOI:
10.1016/j.cplett.2013.03.079

Publication date:
2013

Chemical Physics Letters 571 (2013) 44–48

Contents lists available at SciVerse ScienceDirect

Chemical Physics Letters

journal homepage: www.elsevier.com/locate/cplett

Platinum and palladium on carbon nanotubes: Experimental and theoretical studies

J.J. Adjizian [a], P. De Marco [b], I. Suarez-Martinez [c], A.A. El Mel [b], R. Snyders [b], R.Y.N. Gengler [d], P. Rudolf [d], X. Ke [e], G. Van Tendeloo [e], C. Bittencourt [b], C.P. Ewels [a,*]

[a] IMN, Université de Nantes, CNRS, 2 rue de la Houssinière, BP32229, 44322 Nantes, France
[b] Plasma Surface Interaction Chemistry, University of Mons, Avenue N. Copernic 1, 7000 Mons, Belgium
[c] Nanochemistry Research Institute, Curtin University of Technology, GPO Box U1987, Perth 6845, Western Australia, Australia
[d] Zernike Institute for Advanced Materials, University of Groningen Nijenborgh 4, 9747 AG Groningen, The Netherlands
[e] Electron Microscopy for Material Science, University of Antwerp, Belgium

ARTICLE INFO

Article history:
Received 12 March 2013
In final form 26 March 2013
Available online 6 April 2013

ABSTRACT

Pristine and oxygen plasma functionalised carbon nanotubes (CNTs) were studied after the evaporation of Pt and Pd atoms. High resolution transmission electron microscopy shows the formation of metal nanoparticles at the CNT surface. Oxygen functional groups grafted by the plasma functionalization act as nucleation sites for metal nanoparticles. Analysis of the C1*s* core level spectra reveals that there is no covalent bonding between the Pt or Pd atoms and the CNT surface. Unlike other transition metals such as titanium and copper, neither Pd nor Pt show strong oxygen interaction or surface oxygen scavenging behaviour.

1. Introduction

Research on the physical and chemical properties of carbon nanotubes (CNTs) has been stimulated by extensive reports on their potential use as active component of novel devices [1–5]. In particular, CNTs showing optimal charge transport properties are promising candidates for replacing copper interconnects in nanoelectronics circuits provided that the Schottky barrier that forms at the interface between the CNT surface and the electrical contact can be engineered [6]. Reports on both semiconducting and metallic CNT devices show the influence of the CNT surface chemistry on the contact resistance [7,8]. Electrical contacts to CNTs have been fabricated with different metals and disparities in the resistance have been associated to the presence of oxygen at the CNT surface [9,10]. Metals such as Ti, Cu and Rh were reported to remove the oxygen atoms adsorbed on the CNT surface forming an oxide barrier at the interface CNT-metal contact increasing the contact resistance. In particular, Rh and Cu were reported to scavenge oxygen from oxygenated vacancy sites [11,12]. The removal of the oxygen and formation of the oxide layer by the metal atoms were associated to the easy oxidation of the metal [13]. In this context, Pt and Pd were proposed for electrical contacting carbon nanotubes, with Pd being reported as the best metal giving low contact resistance in most of literature [9,14]. In bulk samples, Pd is known to form a stable oxide, PdO, whereas Pt does not [13]. This difference in chemical reactivity is also likely to manifest at the nanoscale, and in particular suggests that interaction with oxygen will be very important. While there have been previous theoretical investigations of Pt and Pd bulk interaction with carbon nanotubes [15,16], theoretical studies of Pt and Pd interaction with defects are much rarer [17,18]. In this work, in order to investigate the possible removal of oxygen from the CNT surface by platinum and palladium atoms, we perform a comparative study between these two metals when deposited on pristine and oxygen functionalized multi-walled carbon nanotubes. The growth, electronic structure and chemical composition of the metal contact were studied by high resolution transmission electron microscopy (HRTEM), core level photoemission spectroscopy (XPS) and density functional theory (DFT) calculations.

2. Method

Pristine and oxygen plasma functionalized CNTs produced by chemical vapour deposition were used for the experiments. The oxygen plasma functionalization (f_o) was performed in an inductive coupled radio frequency (13.56 MHz) plasma discharge [19]. The carbon nanotubes were exposed during 30 s to oxygen plasma generated at a gas pressure of 0.1 Torr, using 15 W of applied electrical power. Samples for HRTEM and XPS analysis were simultaneously exposed to the plasma. For the HRTEM analysis, the CNTs were dispersed in ethanol and sonicated. A drop of the solution was then deposited onto a honeycomb carbon film supported by a copper grid. To avoid dispersions on the plasma chamber and

* Corresponding author.
E-mail address: chris.ewels@cnrs-imn.fr (C.P. Ewels).

0009-2614/$ - see front matter © 2013 Elsevier B.V. All rights reserved.
http://dx.doi.org/10.1016/j.cplett.2013.03.079

post-treatment contamination, the samples were treated on their support. For the XPS measurements, the CNT powder was supported on a copper conductive tape for ultra high vacuum. Different amounts of Pt and Pd were thermally sublimated onto the CNTs; the amount deposited is reported as the intensity ratio between the Pd $3d_{5/2}$ (or Pt $4f_{7/2}$) and C1*s* core level photoemission signals.

The formation and dispersion of the metal particles at the CNT surface was observed by HRTEM using a Philips CM30-FEG microscope operating at 300 kV.

For the elemental and chemical characterisation of the samples, X-ray photoemission experiments were performed at UE56 beamline BESSY II (Berlin) using the Mustang end-station. The nominal energy resolution (source plus analyser) was 0.1 eV. The Au$4f_{7/2}$ peak at 84.0 eV binding energy recorded on a reference sample, in electrical contact with the Cu tape supporting the CNTs, was used for calibration of the binding energy scale.

Density functional theory (DFT) calculations were performed with the Local Density Approximation (LDA) as coded in the AIMPRO package [20]. The charge density of the supercell was fitted to plane waves with an energy cut-off of 200 Ry. All relativistic pseudopotentials are included via the Hartwigsen–Goedecker–Hutter scheme [21]. Charge density oscillations in part-filled degenerate orbitals during the self-consistency cycle were damped using a Fermi occupation function with kT = 0.04 eV. Atom-centred Gaussian basis functions are used to construct the many-electron wave function with 38 independent functions used for each carbon atom and 50 for each metal atom. A Bloch sum of these functions is performed over the lattice vectors to satisfy the periodic boundary conditions of the supercell. Calculations were performed on a $8 \times 8 \times 1$ unit cell of graphene (C_{128}), with single k-point sampling at (½,½,½). In the analysis that follows, a perfect layer of graphene and isolated metal atom were taken as the standard states of carbon and metal respectively.

3. Results and discussion

Figure 1 shows typical HRTEM images recorded on the samples after deposition of Pt and Pd on the oxygen-functionalized carbon nanotubes (f_o-CNTs). We observe the formation of nanoparticles for both metals. Kuhrt et al. reported that transition metals are mobile and form clusters on the graphite surface, as the cohesive energy of these metals is larger than the adsorption enthalpy [22]. The nucleation centres are chemical or structural defects at the surface of the graphite surface. Considering that both Pt and Pd have been reported to interact with oxygen atoms [22,23], it seems likely that Pt and Pd nanoparticle nucleation could occur in the proximity of oxygenated defects created by the plasma treatment.

The XPS spectra were recorded with a photon energy of 400 eV; the kinetic energy for the photoelectrons emitted from the C1*s* level using this excitation energy is about 115 eV corresponding to an electron mean free path of approximately 10 Å [24]. Thus, the analysis of the C1*s* peak allows evaluating the chemical modifications at the CNT surface due to the oxygen plasma treatment followed by the Pd and Pt deposition.

The C1*s* spectrum recorded on pristine CNTs, originated in sp^2-hybryidized graphite-like carbon atoms, shows an asymmetric main peak centred at 284.4 eV with a tail extended to the higher energy region. This asymmetry has been explained in terms of many-electron interactions in the photoemission process leading to final states where in addition to the emission of the C1*s* electron also low energy electron-hole excitations occur. These final states are also called shake-up feature. After the oxygen plasma functionalization the C1*s* spectrum shows new components at higher binding energies which are attributed to the photoelectrons emitted

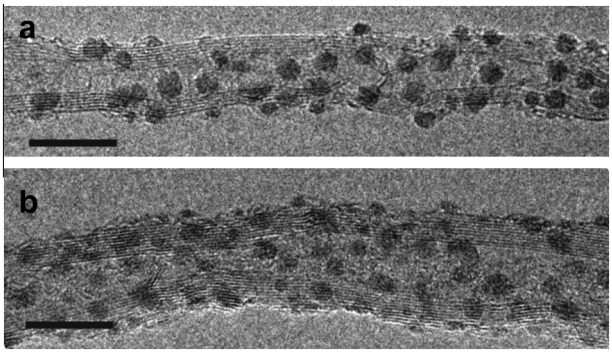

Figure 1. High resolution transmission electron micrographs of (a) Pd and (b) Pt on oxygen plasma-treated carbon nanotubes. (Scale bar corresponds to 10 nm).

from carbon atoms belonging to hydroxyl (component centred at 286.2 eV) and carbonyl (or ether, component centred at 287.2 eV) [25]. After the metal deposition, the absence of additional structures at lower binding energy than the C1*s* peak at 284.4 eV indicates the absence of covalent bonding between the Pt (or Pd) atoms and the CNTs surface (Figure 2) [24].

The metal evaporation causes an increase in the asymmetry of the C 1s peak of both pristine and oxygen plasma functionalized CNTs and a shift of 0.1 eV towards low binding energy, for both metals. Zhu and Kaxiras showed that for a bulk Pd/CNT interface electrons are depleted from both sides of the interface and accumulate between the C and Pd atoms forming the interface [16]. And, that the density of states (DOS) near the Fermi level is larger in the metal decorated CNTs (Pd or Pt decorated) than in the pristine and oxygen treated CNTs. This increase is due to the presence of interface states as well as the d-states from metal atoms which are nearly full due to the depletion of electrons [16].

The width of the asymmetry is set primarily by the DOS near the Fermi energy level, therefore it is suggested that the increase in the asymmetry is due to a larger DOS in both Pd/CNT and Pt/CNT systems.

Density Functional Theory calculations were performed to study the interaction of the metal atoms with the graphene surface. Our calculated binding energy of a single Pd atom to pristine graphene is 2.18 eV, slightly lower than that for Pt at 2.89 eV but nonetheless showing strong adhesion in both cases. The most stable binding site for both metal atoms is above a C-C bond (see Figure 31a and 2a), where Pt atoms sit 1.97 Å above the carbon layer and Pd sits at a height of 1.98 Å. The energy difference with other sites was very small (less than 0.1 eV for sites above a carbon atom and 0.3 eV for sites above hexagon centres). This small energy variations with binding site shows that while the binding energies for isolated atoms are quite high, metal–carbon interaction is very delocalized in both of these systems. Therefore, it is expected that both species will be extremely mobile on the nanotube surface and that any deposited Pd or Pt to rapidly migrate to any available trapping sites.

To explore the metal–carbon interaction further, we optimised four metal atoms on the carbon surface in two different configurations, either arranged in a flat parallelogram parallel to the carbon surface, or in a tetrahedral 'nanoparticle' (see Figure 4). We found the tetrahedral arrangement slightly more stable for both metals, 0.25 eV for the Pd and 0.18 eV for Pt. This indicates a weak driving force for clustering and nanoparticle formation and suggests that these metals will not wet the tube surfaces, in agreement with our HRTEM observations.

We study the interaction of metal atoms with defects on the graphene surface. The interaction with a pristine undecorated vacancy is extremely strong (see Figure 31b and 2b). The isolated metal atom binds to a pristine vacancy with an energy of 6.76 eV for

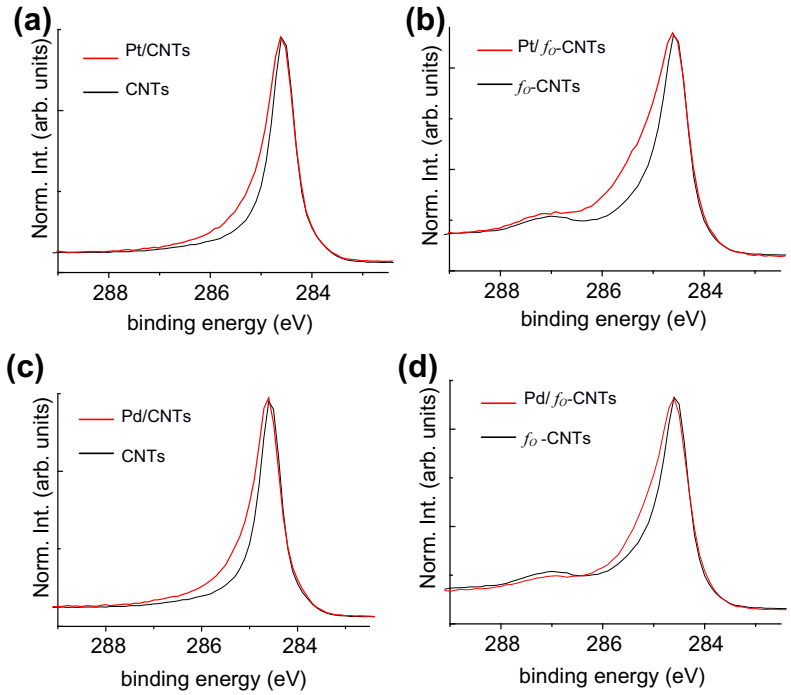

Figure 2. Comparison between the normalised C1*s* peak of (a) pristine CNTs and Pt-decorated (b) f_o-CNTs and Pt-decorated f_o-CNTs (c) pristine CNTs and Pd-decorated CNTs and (d) f_o-CNTs and evaporated Pd on f_o-CNTs. The metal was evaporated simultaneously on pristine CNTs and *fo*-CNTs; the ratio between the area under the Pt4$f_{7/2}$ (Pd 3$d_{5/2}$) peak (not shown here) and the area under the C1*s* peak for both samples was 1.7 (0.03).

Pd and 8.50 eV for Pt, in reasonable agreement with literature values [17]. This means that surface mobile Pd will bind to a vacancy with energy of 4.58 eV, and Pt with 5.61 eV. While these large binding energies suggest that pristine vacancies will be strong trapping sites for both metals, such defects are unlikely to exist since they are highly reactive, notably in the presence of oxygen.

The most common vacancy-related defect in an oxygenated environment is an oxygenated vacancy (Vac-O_2) [19,26], *i.e.* a vacancy with two oxygen atoms, one in a ketone form and, the other in an ether-reconstructed bond. This structure is also consistent with the rather intense XPS peak observed at 287.2 eV assigned to ether and carbonyl groups [19,26]. Once again the calculations show similar binding energies for Pd and Pt, with strong binding of 3.04 eV (3.24 eV) for Pd (Pt), *i.e.* 0.86 eV (0.35 eV) more than to the pristine surface. Thus surface mobile Pd and Pt atoms will trap at Vac-O_2 defects; however this will only serve as a dynamic trap at room temperature. We can estimate trapping time by taking a first order Arhennius hopping model, with attempt frequency of the

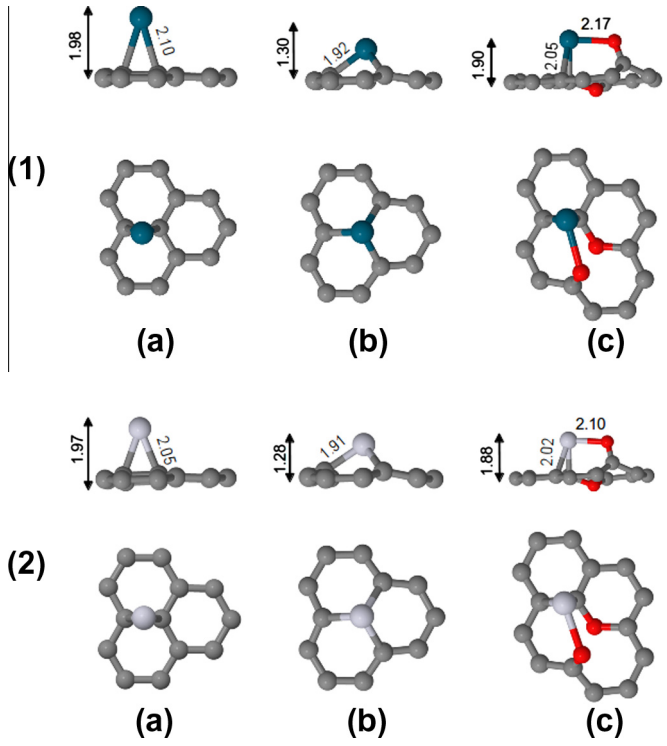

Figure 3. Optimised structures for (1) a Pd and (2) a Pt metal atom on (a) pristine graphene, (b) a vacancy site, (c) an oxygenated vacancy site (vac-O_2). Bond lengths given in Å.

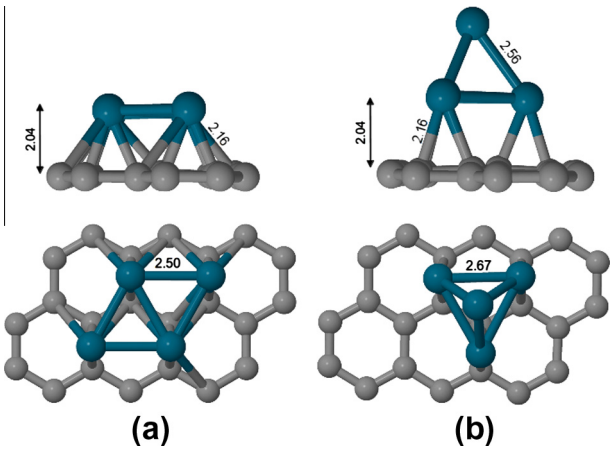

Figure 4. Four Pd metal atoms on the carbon surface in two different configurations: (a) flat parallelogram parallel to the carbon surface, (b) in a tetrahedral 'nanoparticle'. Structure (b) is 0.25 eV more stable showing preference for Pd clustering rather than surface wetting.

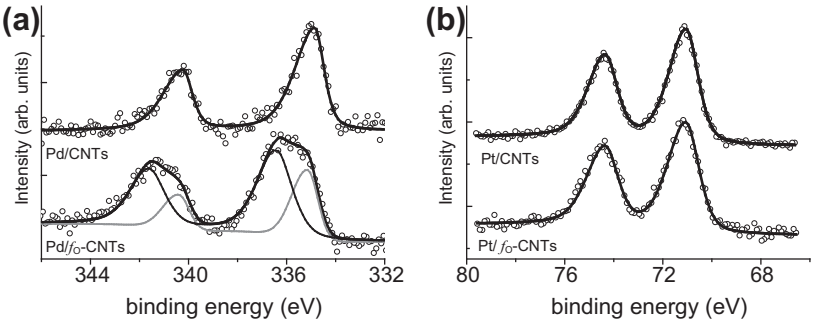

Figure 5. Comparison between the normalised (a) Pd3*d* peak of Pd-decorated pristine and f_o-CNTs (b) Pt4*f* peak of Pt-decorated pristine and f_o-CNTs.

Table 1
Calculated binding energy (eV) and Mulliken charges (e) of Pd and Pt atom on pristine and defective graphene sheets (Vac = carbon vacancy).

Binding site	Binding energy (eV)		Mulliken charge (e)	
	Pd	Pt	Pd	Pt
Pristine	2.18	2.89	+0.348	+0.054
Vac	6.76	8.50	+0.492	+0.233
Vac-O_2	3.04	3.24	+0.499	+0.355

Debye frequency (10^{13} Hz) and ignoring entropic considerations. In such a model a barrier of 0.86 eV implies that at room temperature the trapping time for the single Pd atom at the oxygenated vacancy will be of the order of one minute (around one microsecond for a barrier of 0.35 eV for Pt). The metal atom surface migration barrier will be of the same order as the 0.1 eV energy difference between different binding sites. Given the extremely low surface migration barriers calculated for both species, it seems likely that the metals will spend the majority of their time at oxygenated vacancy trapping sites, with likely interchange of metal between trapping sites facilitating processes such as particle Ostwald ripening [27]. The preferential binding site for both metals to the vacancy is above neighbouring C–C back bonds (see Figure 3c). Placing the metal atom directly on the vacancy site, or other configurations where the metal has displaced one of the oxygen atoms from the vacancy does not give thermodynamically stable structures. Thus unlike other metals we have examined previously such as Ti or Cu [10,12,28], neither Pd or Pt will actively scavenge oxygen from the nanotube surface. The shortest distance between Pd and a C atom for Vac-O_2/Pd is 2.05 Å (2.02 Å for Pt), close to the shortest distance of 2.1 Å (2.05 Å for Pt) in the case of a pristine graphene layer. In both cases the bond is significantly longer than that of palladium carbide, where the Pd–C distance is calculated to be 1.712 Å [29]. Thus we would not expect to see a strong Pd–C interaction in photoelectron spectrum. However the Pd–O bond lengths for Vac-O_2/Pd (2.17 Å) are in the same range as that of PdO, 2.024 Å [30], indicating we might expect palladium oxide type signature in the photoelectron spectrum. These statements are in line with the results shown in Figure 5: after palladium deposition the 3*d* peak shows a new component shifted by approximately 1 eV towards high binding energy this component was reported to be due to the formation of Pd–O bonds. Conversely after platinum evaporation no new components are clearly observed.

Finally, we calculate the Mulliken charges of both Pd and Pt on the pristine and on the defective surface. This is one of the few areas where we see differences in behaviour between Pd and Pt in the calculations. While Pd has a charge state of +0.348e on the pristine surface, Pt shows almost no charge transfer (+0.054e). Charge transfer increases in both cases when carbon vacancies and oxygenated vacancies are present. While the Pt charge state increases to +0.233e/+0.355e in these two cases, it remains lower than that of Pd. These changes can be understood since both the undecorated and oxygen functionalised vacancies are acceptors. The values are summarised in Table 1.

Thus in general, the calculations show a remarkable consistency in behaviour between Pt and Pd on pristine and defective graphene surfaces. Both species rapidly migrate and cluster, binding weakly to oxygenated vacancies without scavenging oxygen from the defects.

There is good convergence between the conclusions from the calculations and the experimental observation via HRTEM and XPS C1*s* spectra. Clustering is predicted and observed, around defect sites. Metal deposition on the untreated nanotubes results in an increased asymmetry of the primary C1*s* peak associated with increased metallicity. This is consistent with the calculated metal–carbon charge transfer and associated increase in density of states at the Fermi level. After oxygen plasma treatment, the nanotubes show a new component in the C1*s* spectrum associated with C–O bonding is observed. In general the invariance of this peak before and after metal deposition confirms the weak metal–oxygen interaction. The weak change in this peak in the Pd case may imply some limited oxygen scavenging, but compared with other transition metal systems the relatively invariant C1*s* spectrum confirms the weak metal-host interaction for both Pt and Pd.

We note that the interaction we observe differs from that of Hull et al. who deposited pre-prepared Pt nanoclusters onto functionalised carbon nanotubes [31]. In this case, while the majority of the Pt was present in metallic form, they observed a weak XPS signal indicating PtO_x formation on the nanocluster surfaces. It seems that the oxygen concentration and the structure at the surface of the particles is important, since they found that lower oxygen concentrations did not result in Pt nanoparticle binding. FTIR (Fourier transform infrared spectroscopy) observations showed peak shifts for both carbonyl and ether groups consistent with our findings here of significant metal interaction with the defect sites [31].

4. Conclusions

The deposition of both Pt and Pd atoms on the pristine and oxygen functionalized CNTs resulted in the formation of small clusters as revealed by HRTEM. XPS analysis performed in order to evaluate the chemical changes at the CNT sample due to the oxygen plasma treatment followed by Pt or Pd deposition, shows that there is no covalent bonding between the Pt or Pd atoms and the oxygenated sites created on the CNT surface by the plasma exposition. Both the metal cluster formation and the type of bonding were confirmed by DFT modelling.

Acknowledgement

This work is supported by the Belgian Fund for Scientific Research (FRS-FNRS) under FRFC contract 'Chemographene' (convention N°2.4577.11) and by the European Community—Research Infrastructure Action under the FP6 'Structuring the European Research Area' Programme through the Integrated Infrastructure Initiative' Integrating Activity on Synchroton and Free Electron Laser Science—Contract R II 3-CT2004-506008 (IASFS). X. Ke and G. Van Tendeloo are grateful to the funding from the European Research Council under the 7th Framework Program (FP7), ERC grant N°246791 – COUNTATOMS. Support from the COST action MP0901 'NanoTP', ARC-UMONS 'COLD Plasma' are gratefully acknowledged and the 'Top Research School' program of the Zernike Institute for Advanced Materials under the Bonus Incentive Scheme (BIS) of the Netherlands' Ministry of Education, Science, and Culture.

References

[1] M. Chen, X. Song, S. Liu, Z. Gan, Q. Lv, Microsyst. Technol. 18 (2012) 679.
[2] Y.J. Huang, H.C. Wu, N.H. Tai, T.W. Wang, Small 8 (2012) 2869.
[3] S. Huang et al., J. Mater. Chem. 22 (2012) 16833.
[4] H. Wang, J. Luo, F. Schäffel, M.H. Rümmeli, G.A.D. Briggs, J.H. Warner, Nanotechnology (2011) 22.
[5] F. Yang, L. Hu, H. Lin, L. Zheng, T. Guo, Zhenkong Kexue yu Jishu Xuebao/J. Vacuum Sci. Technol. 32 (2012) 192.
[6] N. Chiodarelli et al., Microelectron. Eng. 88 (2011) 837.
[7] Y. Chai, A. Hazeghi, K. Takei, H.Y. Chen, P.C.H. Chan, A. Javey, H.S.P. Wong, IEEE Trans. Electron Devices 59 (2012) 12.
[8] A. Javey, R. Tu, D.B. Farmer, J. Guo, R.G. Gordon, H. Dai, Nano Lett. 5 (2005) 345.
[9] A.A. Kane et al., Nano Lett. 9 (2009) 3586.
[10] A. Felten et al., ChemPhysChem 10 (2009) 1799.
[11] I. Suarez-Martinez et al., ACS Nano 4 (2010) 1680.
[12] C. Bittencourt, X. Ke, G. Van Tendeloo, S. Thiess, W. Drube, J. Ghijsen, C.P. Ewels, Chem. Phys. Lett. 535 (2012) 80.
[13] A. Kanda, Y. Ootuka, K. Tsukagoshi, Y. Aoyagi, Appl. Phys. Lett. 79 (2001) 1354.
[14] A. Javey, J. Guo, Q. Wang, M. Lundstrom, H. Dai, Nature 424 (2003) 654.
[15] V. Vitale, A. Curioni, W. Andreoni, J. Am. Chem. Soc. 130 (2008) 5848.
[16] W. Zhu, E. Kaxiras, Phys. Status Solidi B 243 (2006) 2164.
[17] A.V. Krasheninnikov, P.O. Lehtinen, A.S. Foster, P. Pyykkö, R.M. Nieminen, Phys. Rev. Lett. (2009) 102.
[18] I. Suarez-Martinez, A. Felten, J.J. Pireaux, C. Bittencourt, C.P. Ewels, J. Nanosci. Nanotechnol. 9 (2009) 6171.
[19] A. Felten, C. Bittencourt, J.J. Pireaux, G. Van Lier, J.C. Charlier, J. Appl. Phys. (2005) 98.
[20] P.R. Briddon, M.J. Rayson, Phys Status Solidi B 248 (2011) 1309.
[21] C. Hartwigsen, S. Goedecker, J. Hutter, Phys. Rev. B Condens. Matter Mater. Phys. 58 (1998) 3641.
[22] C. Kuhrt, M. Harsdorff, Surf. Sci. 245 (1991) 173.
[23] L.R. Saenz, P.B. Balbuena, J.M. Seminario, J. Phys. Chem. A 110 (2006) 11968.
[24] F. Reinert, S. HÃ¼fner, New J. Phys. (2005) 7.
[25] C. Bittencourt et al., J. Phys. Chem. C 115 (2011) 20412.
[26] J.C. Charlier et al., Nanotechnology 20 (2009) 375501.
[27] C.T. Campbell, Surf. Sci. Rep. 27 (1997) 1.
[28] A. Felten, C. Bittencourt, J.F. Colomer, G. Van Tendeloo, J.J. Pireaux, Carbon 45 (2007) 110.
[29] R.S. DaBell, R.G. Meyer, M.D. Morse, J. Chem. Phys. 114 (2001) 2938.
[30] J.R. McBride, K.C. Hass, W.H. Weber, Phys. Rev. B 44 (1991) 5016.
[31] R.V. Hull, L. Li, Y. Xing, C.C. Chusuei, Chem. Mater. 18 (2006) 1780.